Characterization of Electrically Conductive Polymers Integrated in Additively Manufactured Parts for Sensing

Available online at www.eccomasproceedia.org
Eccomas Proceedia SMART (2025) 1270-1281

ECCOMAS Proceedia

XI ECCOMAS Thematic Conference on Smart Structures and Materials - SMART 2025
M. Krommer, M. Nader and M. Schagerl (Eds)

Received: 27 March 2025 / Revised: 30 August 2025 / Accepted: 20 September 2025


# Characterization of Electrically Conductive Polymers Integrated in Additively Manufactured Parts for Sensing

Giorgio De Pasquale, Ferdinando Ursi

**Abstract**. Additive Manufacturing (AM) technologies enable the layer-by-layer fabrication of complex geometries with advantages such as cost-effectiveness, waste reduction, and design flexibility. Among polymer-based AM techniques, fused deposition modeling (FDM) is widely used due to its affordability and ease of use. The demand for high-performance materials has led to the development of polymer matrix composites (PMCs), including conductive polymer composites (CPCs), which integrate electrically conductive fillers within a polymeric matrix. CPCs, particularly those with carbon-based fillers, offer promising applications in sensing devices and 3D-printed electronics.
This study investigates commercial CPCs for strain sensing applications, focusing on the impact of sensor track width and temperature on functional performance. Two CPCs are analyzed: a graphite-filled TPU-based CPC (Fili) and a carbon-black-filled TPU-based CPC (FilaFlex Conductive). The materials are co-printed on PLA-based substrates using a dual-extruder FDM process. Tensile tests reveal that graphite-filled CPCs exhibit a strong linear piezoresistive response, while carbon-black-filled CPCs show lower strain sensitivity. Additionally, thermal characterization demonstrates that both CPCs exhibit a positive temperature coefficient (PTC), though matrix-filler interactions influences their response at higher temperatures.
The results indicate that graphite-based CPCs are suitable for strain sensing due to their linear piezoresistive behavior, while carbon-black-filled CPCs maintain electrical stability under mechanical deformation. These findings provide valuable insights for selecting CPCs in sensor applications and highlight the need for further studies on repeatability and strain limits.

**Key words**: Conductive polymer composites (CPCs), Nanomaterials, Additive Manufacturing, Sensors, IoT.

## 1 INTRODUCTION

Additive manufacturing (AM) technologies encompass all methods capable of creating objects by building them layer by layer. These technologies offer several advantages, including the ability to produce complex geometries, cost-effectiveness, waste reduction, and design flexibility. However, they also present challenges such as the frequent need for post-processing, design inaccuracies, and a limited selection of available materials [1], [2].

Giorgio De Pasquale & Ferdinando Ursi
Smart Structures and Systems Lab, Politecnico di Torino, Department of Mechanical and Aerospace Engineering, 10129 Torino, Italy. e-mail: giorgio.depasquale@polito.it

ISSN:3078-543X. Published by Eccomas Proceedia.
Peer-review under responsibility of the organizing committee of SMART 2025.
doi: 10.7712/150125.13721.305001

During the printing process, the bonding mechanism between layers depends on both the material class (e.g., metal, polymer, or ceramic) and the form of the raw material or feedstock (e.g., powder, liquid, filament, or pellet). AM technologies are widely used across various industries, including medical, manufacturing, aerospace, and automotive sectors showing also. Metals and alloys are commonly employed in applications requiring load-bearing capabilities, heat resistance, or thermal management, thanks to their superior mechanical and thermal properties [3].

Among the new trends regarding the AM technology, efforts also focus on the development of metamaterials [4], [5], [6] and the integration of AM processes with existing methods, such as combining metal AM with carbon composite processes [7], [8], [9], [10] or the integration of sensors in AM components [11]. On the other hand, the primary limitation of metal-based AM is the relatively high cost, which led to the increasing popularity of polymer-based AM, despite its relatively lower mechanical performance. Among polymer-based AM techniques, fused deposition modeling (FDM) is the most widely adopted due to its cost-effectiveness, accessibility to feedstocks, and ease of use. The FDM process involves the extrusion of molten thermoplastic material through a heated nozzle. Traditionally, materials such as polylactic acid (PLA) and acrylonitrile-butadiene-styrene (ABS) are commonly used. However, the growing demand for high-performance materials has led to the development of the new feedstock class of polymer matrix composites (PMC) [12]. In PMCs, the mixing of a polymeric matrix with a filler material enhances the material properties. While the polymeric matrix provides the material with good extrudability, the filler material enhances one or more of the material properties.

Carbon-fiber-reinforced-polymers (CFRP) is one of the most relevant PMC in which the use of continuous carbon fibers as filler material results in a significant increase in mechanical properties that at times may compete with the one of metal parts [13], [14]. In the last years, relevant efforts have been spent in the exploration of conductive polymer composites (CPCs), a class of materials in which the matrix is the structural component and the filler, who exhibits electrically conductive properties, is the functional part. Polymeric matrices are classified in hydrogels, synthetic polymers, natural rubber and synthetic rubber; the fillers are classified in carbon-based, metallic, emerging materials and intrinsically conductive polymers [15]. The CPCs based on carbon and metallic fillers are also referred to as conductive polymer nanocomposites because they are dispersed in the matrix in the form of nanoparticles (NPs) [16], [17]. Even though the metal nanoparticles such as gold, silver or copper NPs noticeably enhance the CPCs electrical properties, they are generally expensive and often cause clogging during the deposition process [18]. The carbon-based NPs deployed in CPCs can be distinguished in carbon black (CB), carbon nanotubes (CNTs) and graphite particles (GPs), characterized by a different aspect ratio and sometime referred to as 0D, 1D and 2D NPs, respectively [18], [19], [20].

The electrical conduction in the CPC is described by the percolation theory, in which the electrical charges move from one nanoparticle to another when they are in contact or very close. Hence, the percolation occur when the volume content of the filler in the CPC is higher than the percolation threshold [20], [21]. The percolation threshold depends on a number of filler parameters including the aspect ratio, the filler size and the filler size distribution [18].

Nowadays, despite CPCs are treated with several processes including inkjet, aerosol jet printing (AJP) and electrohydrodynamic jet printing (EHD), the most simple AM technology to process CPCs is the FDM because it shows less clogging issues [22]. CPCs find wide application in several fields such as automotive, aerospace [23], biomedicine [24], [25], shielding [26], sensing devices [27], [28], [29], [30] and, more generally, in the 3D-printed electronics.

The interconnection between components, a cornerstone of the internet of things (IoT), and the increasing demand for data to train artificial intelligence (AI) models are relevant aspects. In this context, the widespread adoption of this class of materials offers a significant opportunity to address the growing need for data.

In literature, many studies have been reported on the enhancement of the electrical properties of CPCs. However, the development of custom-tailored materials is often complex, challenging to replicate, and requires meticulous manufacturing processes [31]. Additionally, the limited number of CPC's producers rarely provide information on their suitability as sensing materials. To the best of the authors' knowledge, no prior study has specifically investigated this aspect. The experimental characterization of commercial CPCs can therefore provide valuable insights, enabling informed material selection, both for the design of new CPCs and for their procurement. This research aims to introduce and analyze key parameters of selected commercial carbon-based CPCs for strain sensing applications, while also examining how the thickness of the sensing device affects its functional performance. Additionally, the pyro resistive response of the CPCs is investigated to establish the impact of temperature on its sensing performances.

## 2 SAMPLES AND TESTS DESCRIPTION

### 2.1 Materials

Literature emphasizes that stretchability, or the ability to generate large strain values, is a key factor for strain sensing. One major challenge associated to stretchability is the decohesion between the sensing material and the substrate. To improve the stretchability of the sensor, the sensing structure is co-printed with the specimen using a double extruder, ensuring it stays securely attached to the substrate during testing.

Polymeric matrices known for their excellent stretchability include hydrogel, SEBS, PDMS, and Ecoflex, with TPU being the most affordable and widely used option [32].

The CPCs selected for characterization are:

- "Fili" – a TPU-based CPC filled with graphite particles, manufactured by AIMPLAS Technological Institute of Plastics.
- "FilaFlex Conductive" – a TPU-based CPC filled with carbon black (CB), manufactured by Recreus Industries.

The substrate used for the CPCs in this study is a dog-bone specimen compliant with the ASTM D638 Type V standard, made from PLA Pro1 white by BASF.

### 2.2 Specimens preparation

The sample batch is manufactured with the double extruder FDM printer UltiMaker S5. Connecting the CPC to the measurement apparatus with silver inks is a consolidated operation observed in several studies [31], [33]. However, these inks require careful handling, making them unsuitable for long-term applications. To address this limitation, a more reliable connection method is proposed, based on the embedding of copper electrodes using a stop-and-resume technique during the printing process, ensuring a stable sensor connection.

The geometry of the sensing device and substrate is designed in SolidWorks and then exported as an STL file to the UltiMaker Cura Enterprise slicer software. This software not only allows for setting the printing parameters but also enables precise placement of the sensor and electrodes within the substrate material.

Additionally, this study examines the impact of sensing track width on the sensing properties of CPCs. To evaluate this, CPC-based sensors are printed with three layers of CPC material at widths of 0.4 mm, 0.8 mm, and 1.6 mm.

To assess the tensile behavior of the substrate material, three specimens without CPC are prepared for tensile testing. Furthermore, for each CPC and sensor trace width combination, three specimens are produced for piezoresistive characterization, along with an additional specimen designated for pyro resistive characterization.

### 2.3 Tensile characterization

The tensile test (Figure 1.a), is performed using the INSTRON 8801 universal testing machine under strain rate control conditions at a rate of 1 mm/min. Before testing, the cross-section of the narrowed section of the specimens is measured at three points using a vernier caliper.

The applied load is measured with a 100 kN load cell, while strain is recorded using the uniaxial dynamic extensometer. Since the investigation focuses on the behavior of CPC within the elastic deformation range of the substrate, the test imposes a load range of 0–400 N.

Strain and load signals are acquired by the cRIO-9054 DAQ system, which also records the resistance signal generated by the CPC. The DAQ system synchronizes all signals at a sampling frequency of 100 Hz and transfers the data to a PC for storage and post-processing.

Post-processing is carried out using MATLAB to assess the impact of co-printing the sensor within the dog-bone specimen on the tensile elastic modulus (*E*), or Young's modulus, of the material in the elastic deformation field, defined as:

$$E = \sigma/\varepsilon \tag{1}$$

where $\sigma$ [MPa] represents the normal stress induced in the tensile specimen due to the applied load, and $\varepsilon$ [-] denotes the strain experienced by the specimen as a result of this load.

The strain sensing properties of the CPC are then evaluated by determining their sensitivity to strain, quantified through the strain sensitivity or gauge factor (*GF*), along with the coefficient of determination ($R^2$), which indicates the correlation between the experimental data and a linear regression model. The gauge factor is

$$GF = \frac{\Delta R / R_0}{\varepsilon} \quad (2)$$

where $R_0$ [$k\Omega$] represents the electrical resistance of the CPC before starting the tensile test and $\Delta R$ [$k\Omega$] represents the change in electrical resistance due to the applied load. The coefficient of determination is

$$R^2 = 1 - \frac{\sum_{i=1}^{n} (Y_i - \widehat{Y}_i)^2}{\sum_{i=1}^{n} (Y_i - \overline{Y})^2} \quad (3)$$

where Y refers to the experimental data, $\widehat{Y}$ refers to the linear regression model and $\overline{Y}$ refers to the mean value of all the experimental data.

## 2.4 Thermal characterization

The thermal test (Figure 1.b) is conducted using a feedback controlled heating plate. In literature, thermal investigations reach up to 50 °C[34], thus some it may result useful to assess the thermal behaviour of CPCs under more severe conditions. The applied thermal profile consists in heating the specimens up to the nominal temperature of 140° for 5 hours. Afterward, the heating platform is turned off and the electrical behavior of the CPC during the cooling is sampled for 1 hour.

During the thermal test, the actual temperature on the heating platform, recorded with a K-type thermocouple, and the electrical resistance of the CPC are synchronized and sampled at 100 Hz with the cRIO-9054 DAQ system. The gathered data are sent to the PC and processed on MATLAB.

The output of the test are the thermos-electric characteristics of examined CPCs with track width of 0.4 mm, 0.8 mm and 1.6 mm and the quantification of the degree of thermal hysteresis ($H_T$) during the test:

$$H_T = |A_H - A_C| / A_H \quad (4)$$

where $A_H$ and $A_C$ represents the area under the heating and cooling path.

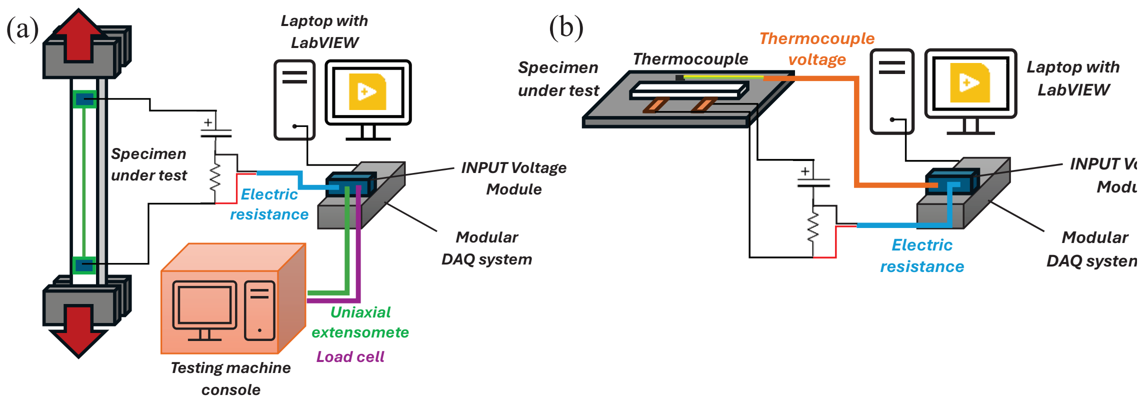


**Figure 1:** Visual representation of the tensile characterization (a) and thermal characterization (b) experimental setup.

## 3 RESULTS AND DISCUSSION

### 3.1 Tensile characterization

The computation of the elastic modulus, based on equation (1), reveals that integrating the sensing apparatus into the substrate affects its tensile response in the elastic region. When the integrated track is small, the elastic modulus significantly increases, regardless of the CPC. This trend is attributed to the surrounding sensor area being reinforced by a wall contour, which contributes to the overall stiffness of the printed part [35]. However, as the CPC cross-section increases, the elastic modulus decreases for both CPCs due to the replacement of the substrate material with more compliant materials. The more pronounced drop in the elastic modulus for FilaFlex Conductive can be attributed to the CB filler's lower load transfer capability compared to the graphite particles in Fili.

Regardless of the sensing track width, Fili exhibits a linear relationship with strain (Figure 2.a), whereas FilaFlex Conductive, as also reported by other authors [36], displays an inconsistent piezoresistive response (Figure 2.b).

The sensing parameters, calculated using equations (2) and (3) and summarized in Table 2, show that Fili demonstrates strong strain-sensing capabilities, with a strain sensitivity exceeding 100 and a coefficient of determination above 0.90. Additionally, increasing the sensing track width further enhances these metrics.

Conversely, FilaFlex Conductive exhibits poor strain-sensing properties, characterized by low strain sensitivity and non-linearity. This behavior is attributed to the aspect ratio of the filler material. Fili contains graphite, which gradually lose contact during matrix deformation due to relative slipping between particles. In contrast, CB, undergoes less predictable changes in particle network percolation during deformation. This comparison highlights that Fili filament provides a sensing material with a linear piezoresistive response, while FilaFlex Conductive is better suited for electronic applications where maintaining electrical properties despite mechanical deformation is crucial. However, the variability in the measured gauge factor limits its potential for large-scale applications.

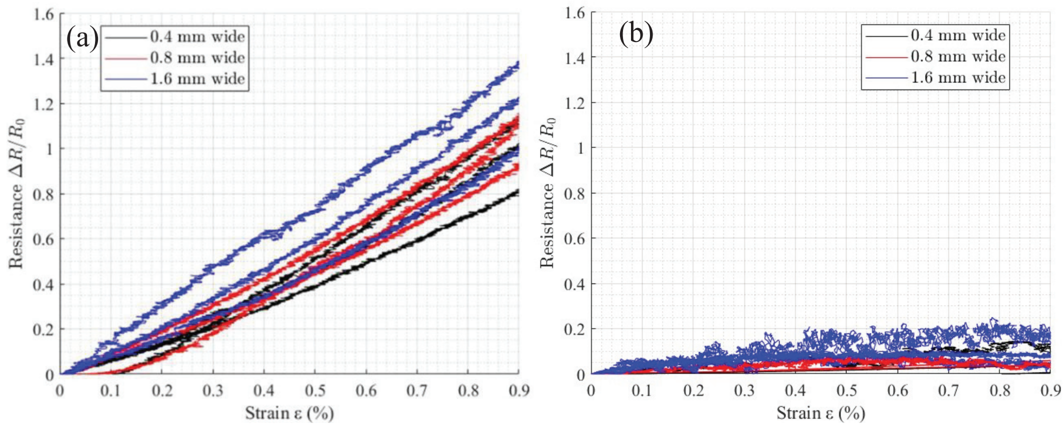


**Figure 2:** Piezoresistive response of Fili (a) and FilaFlex Conductive (b).

**Table 1**: Young's modulus of the dog-bone specimens.

| Track width (mm) | Young's modulus $E$ (MPa) | | |
|---|---|---|---|
| | Fili | FilaFlex Conductive | Without CPCs |
| 0.4 | 2296 | 2261 | 2196 |
| 0.8 | 2202 | 2058 | |
| 1.6 | 2150 | 2000 | |

**Table 2**: Strain sensing metrics of the CPCs.

| Track width (mm) | Strain Gauge $GF$ (-) | | Coefficient of determination $R^2$ (-) | |
|---|---|---|---|---|
| | Fili | FilaFlex Conductive | Fili | FilaFlex Conductive |
| 0.4 | 117 | 6 | 0.96 | 0.72 |
| 0.8 | 122 | 4 | 0.96 | 0.69 |
| 1.6 | 130 | 2 | 0.97 | 0.16 |

## 3.2 Thermal characterization

The pyroresistive response of the CPCs during a heating cycle, as shown in Figure 3, reveals distinct relationships between resistance and temperature, both influenced by the type of nanofiller used.

Fili exhibits a proportional increase in resistance as temperature rises (Figure 3.a). This behavior, known in the literature as a positive temperature coefficient (PTC) effect and in CPCs is due to the matrix thermal expansion [20], [37] , follows a linear trend up to 50°C, after which the CPC experiences a resistance drop. During cooling, the resistance increases again, ultimately leading to a permanent change in electrical resistance at the end of the test.

In contrast, FilaFlex Conductive (Figure 3.b) also demonstrates a PTC effect, with an initial plateau followed by a linear increase in resistance up to 90°C. Similar to Fili, the resistance then drops. However, unlike Fili, FilaFlex Conductive continues to experience a resistance drop during cooling, suggesting that CB particles enhance their conductivity properties after the heat cycle.

These pyroresistive behaviors can be attributed to differences in the aspect ratio of the fillers and, more specifically, to the filler-matrix interactions, as permanent matrix deformations lead to lasting alterations in sensing characteristics [20]. The test results indicate that when using graphite-filled CPCs for sensing applications, operating temperature must be carefully considered, as exceeding 50°C may alter sensing properties. In contrast, CB-filled CPCs exhibit improved conductivity after the heating cycle, suggesting that controlled heat exposure could serve as a strategy to enhance the resistance properties of this material class.

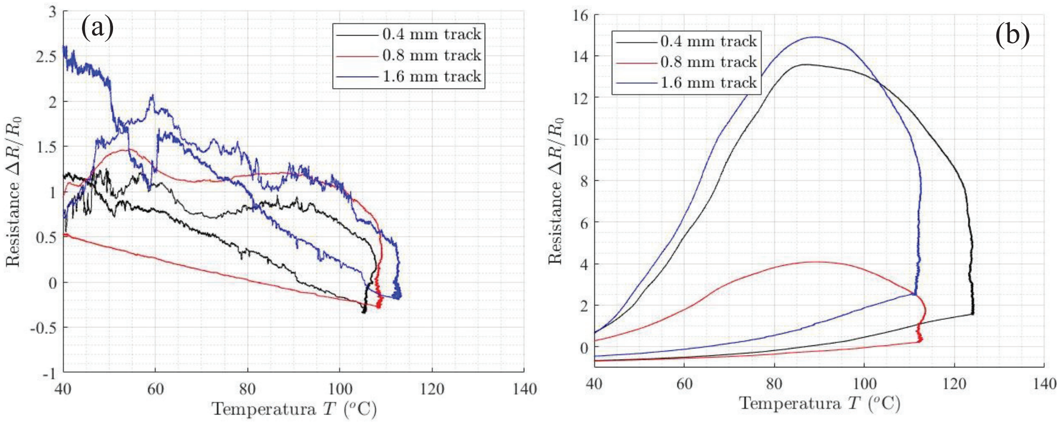


**Figure 3**: Pyroresistive response of Fili (a) and FilaFlex Conductive (b) with a 1.6 mm sensing track.

The hysteretic observed in Figure 3 over the heat cycle and formalized with the equation (4) are reported in Table 3.

**Table 3**: Thermal hysteresis of the CPCs.

| Track width (mm) | Thermal hysteresis $H_T$ (-) | |
|---|---|---|
| | Fili | FilaFlex Conductive |
| 0.4 | 0.257 | 0.891 |
| 0.8 | 0.514 | 0.826 |
| 1.6 | 0.189 | 0.850 |

The thermal hysteresis aligns with the curve in Figure 3 as the CB-based CPC (FilaFlex Conductive) exhibits a stable hysteresis of approximately 0.85, while the graphite-based CPC (Fili) shows more variability. However, no clear scale effect is observed with increasing track width. This trend can be attributed to the significant influence of process variability on the final properties of the CPC.

## 4 CONCLUSIONS

The analysis conducted has emphasized several important aspects, detailed below.

- Embedding the sensor within the component to be monitored, or more generally into the substrate, alters the tensile properties of the final component. This factor must be carefully considered during the design phase of the sensor section.
- The aspect ratio of the filler significantly affects both the piezoresistive and pyroelectric response of CPCs. The study revealed that graphite-based CPCs demonstrate a strong piezoresistive response, whereas CB-based CPCs (carbon black) exhibit low sensitivity to applied deformation. These behaviors can be crucial in applications where correlating or decorrelating electrical resistance with mechanical strain is required. As with traditional strain gauges, the effect of temperature on resistance must be carefully considered to ensure that the operating temperature does not cause permanent

alterations in the sensor's resistive response.

- The pyroresistive response indicates that both carbon-based CPCs exhibit a positive temperature coefficient (PTC). However, at high temperatures, the matrix-filler interactions affect this relationship. The CB-based CPC demonstrates more stable behavior compared to the graphite-filled counterpart. It is important to note that up to 50°C, graphite-based conductive materials maintain a proportional pyroresistive response.
- The findings confirm that commercial CPCs can be effectively used for suitable strain sensing. When comparing graphite-filled and CB-filled CPCs, the former provides a linear piezoresistive response, making it well-suited for strain sensing applications, while the latter shows low piezoresistive sensitivity, making it preferable for applications where minimizing sensitivity to deformation is desired.
  Depending on the filler used, high temperatures may cause a permanent decrease in electrical resistance, revealing potential strategies for enhancing CPC performance.

In conclusion, the choice of filler plays a crucial role in determining the sensor's properties. Therefore, during CPC selection or design, a thorough evaluation of the filler material is essential.
A comprehensive analysis of the lifetime of resettable sensors is beyond the scope of this study; however, it remains a crucial area for future research. Further investigation into CPC sensing properties should prioritize examining the repeatability of piezoresistive and pyroelectric responses, as well as identifying the maximum strain range where linear correlations hold.

## 5 FUNDING

This paper was funded by the Horizon Europe grant "HORIZON-CL4-2022-RESILIENCE-01", Project MIMOSA (Project 101091826).

## REFERENCES

[1] P. Awasthi and S. S. Banerjee, "Fused deposition modeling of thermoplastic elastomeric materials: Challenges and opportunities," *Addit Manuf*, vol. 46, p. 102177, Oct. 2021, doi: 10.1016/J.ADDMA.2021.102177.

[2] M. Askari *et al.*, "Additive manufacturing of metamaterials: A review," *Addit Manuf*, vol. 36, p. 101562, Dec. 2020, doi: 10.1016/J.ADDMA.2020.101562.

[3] M. Srivastava *et al.*, "Additive manufacturing of Titanium alloy for aerospace applications: Insights into the process, microstructure, and mechanical properties," *Appl Mater Today*, vol. 41, p. 102481, Dec. 2024, doi: 10.1016/J.APMT.2024.102481.

[4] Z. Zeng *et al.*, “Additive manufacturing of metallic metamaterials with enhanced mechanical properties enabled by microstructural and structural design,” *Int J Mach Tools Manuf*, vol. 199, p. 104172, Jun. 2024, doi: 10.1016/J.IJMACHTOOLS.2024.104172.
[5] X. Wu, H. Yan, Y. Zhou, P. Zhang, Q. Lu, and H. Shi, “Review of additive manufactured metallic metamaterials: Design, fabrication, property and application,” *Opt Laser Technol*, vol. 182, p. 112066, Apr. 2025, doi: 10.1016/J.OPTLASTEC.2024.112066.
[6] S. Dai, K. Zhu, S. Wang, and Z. Deng, “Additively manufactured materials: A critical review on their anisotropic mechanical properties and modeling methods,” *J Manuf Process*, vol. 141, pp. 789–814, May 2025, doi: 10.1016/J.JMAPRO.2025.02.038.
[7] G. De Pasquale and A. Coluccia, “Modeling and Experimental Validation of CFRP–Metal Joints Utilizing 3D Additively Manufactured Anchors,” *J Manuf Sci Eng*, vol. 145, no. 11, Aug. 2023, doi: 10.1115/1.4063110.
[8] G. De Pasquale, F. Enes Altunok, and F. Ursi, “Investigation of the Mechanical Strength of CFRP with Co-Cured Additively Manufactured Metal Inserts,” *Procedia Structural Integrity*, vol. 47, pp. 573–578, Jan. 2023, doi: 10.1016/J.PROSTR.2023.07.067.
[9] F. E. Altunok and G. De Pasquale, “Numerical Cohesive Zone Modeling (CZM) of Self-Anchoring AM Metal-CFRP joints,” *Frattura ed Integrità Strutturale*, vol. 18, no. 68, pp. 280–295, Apr. 2024, doi: 10.3221/IGF-ESIS.68.19.
[10] G. De Pasquale and F. E. Altunok, “Multiphase modeling of matrix/fiber-related damaging mechanism in multimaterial additively manufactured joints with 3D interlocking,” *Eng Fail Anal*, vol. 170, Mar. 2025, doi: 10.1016/J.ENGFAILANAL.2025.109272.
[11] G. De Pasquale, “THERMAL MONITORING OF BRAKING SYSTEMS USING METAL AM CALIPERS WITH INTEGRATED SENSORS,” pp. 434–445, Sep. 2023, doi: 10.7712/150123.9798.445855.
[12] X. Wang, M. Jiang, Z. Zhou, J. Gou, and D. Hui, “3D printing of polymer matrix composites: A review and prospective,” *Compos B Eng*, vol. 110, pp. 442–458, Feb. 2017, doi: 10.1016/J.COMPOSITESB.2016.11.034.
[13] A. Sola and A. Trinchi, “The need for fused deposition modeling of composite materials,” *Fused Deposition Modeling of Composite Materials*, pp. 39–89, Jan. 2023, doi: 10.1016/B978-0-323-98823-0.00004-4.
[14] G. De Pasquale and F. Ursi, “Multi-material fittings with carbon fiber reinforcement from AM process: design and characterization,” in *3rd Int. Symp. on Industrial Engineering and Automation (ISIEA)*, Bolzano (Italy), Jun. 2024.
[15] H. T. Tazwar, M. F. Antora, I. Nowroj, and A. Bin Rashid, “Conductive Polymer Composites in Soft Robotics, Flexible Sensors and Energy Storage: Fabrication, Applications and Challenges,” *Biosens Bioelectron X*, p. 100597, Feb. 2025, doi: 10.1016/J.BIOSX.2025.100597.

[16] K. R. Ryan, M. P. Down, N. J. Hurst, E. M. Keefe, and C. E. Banks, “Additive manufacturing (3D printing) of electrically conductive polymers and polymer nanocomposites and their applications,” *eScience*, vol. 2, no. 4, pp. 365–381, Jul. 2022, doi: 10.1016/J.ESCI.2022.07.003.

[17] M. N. Khatun *et al.*, “Sensors based on polymer nanomaterials,” *Sensory Polymers*, pp. 391–428, Jan. 2024, doi: 10.1016/B978-0-443-13394-7.00010-0.

[18] D. Pejak Simunec and A. Sola, “Emerging Research in Conductive Materials for Fused Filament Fabrication: A Critical Review,” *Adv Eng Mater*, vol. 24, no. 7, p. 2101476, Jul. 2022, doi: 10.1002/ADEM.202101476.

[19] A. C. Ezika, H. C. Oyeoka, C. C. Obi, S. C. Ugwu, and M. E. Ibenta, “Enhancing the mechanical and electrical properties of polymers using graphene,” *Polymers and Two-Dimensional Nanocomposites*, pp. 209–261, Jan. 2025, doi: 10.1016/B978-0-443-14131-7.00009-2.

[20] A. del Bosque, X. F. Sánchez-Romate, M. Sánchez, and A. Ureña, “Toward flexible piezoresistive strain sensors based on polymer nanocomposites: a review on fundamentals, performance, and applications,” *Nanotechnology*, vol. 35, no. 29, p. 292003, Jul. 2024, doi: 10.1088/1361-6528/ad3e87.

[21] Z. Wang, J. Zhang, and G. J. Weng, “Modeling the percolation behavior of conductive particles/insulating polymer-based composites with equivalent circuit of resistance,” *Polymer (Guildf)*, p. 128262, Mar. 2025, doi: 10.1016/J.POLYMER.2025.128262.

[22] H. W. Tan, Y. Y. C. Choong, C. N. Kuo, H. Y. Low, and C. K. Chua, “3D printed electronics: Processes, materials and future trends,” *Prog Mater Sci*, vol. 127, p. 100945, Jun. 2022, doi: 10.1016/J.PMATSCI.2022.100945.

[23] A. H. Alami *et al.*, “Additive manufacturing in the aerospace and automotive industries: Recent trends and role in achieving sustainable development goals,” *Ain Shams Engineering Journal*, vol. 14, no. 11, p. 102516, Nov. 2023, doi: 10.1016/J.ASEJ.2023.102516.

[24] N. H. Solangi, R. R. Karri, N. M. Mubarak, and S. A. Mazari, “Mechanism of polymer composite-based nanomaterial for biomedical applications,” *Advanced Industrial and Engineering Polymer Research*, vol. 7, no. 1, pp. 1–19, Jan. 2024, doi: 10.1016/J.AIEPR.2023.09.002.

[25] H. Wang *et al.*, “Comprehensive Study of Mechanical, Electrical and Biological Properties of Conductive Polymer Composites for Medical Applications through Additive Manufacturing,” 2024, doi: 10.3390/polym16182625.

[26] Y. Mamunya *et al.*, “Influence of conductive nano- and microfiller distribution on electrical conductivity and EMI shielding properties of polymer/carbon composites,” *Compos Sci Technol*, vol. 170, pp. 51–59, Jan. 2019, doi: 10.1016/J.COMPSCITECH.2018.11.037.

[27] R. Mutlu, D. Singh, C. Tawk, and E. Sariyildiz, “A 3D-Printed Soft Haptic Device with Built-in Force Sensing Delivering Bio-Mimicked Feedback,” 2023, doi: 10.3390/biomimetics8010127.

[28] X. Xosé Fernández Sánchez-Romate, A. Del Bosque García, M. Sánchez, and A. Ureñ, “Electrical Transport Mechanisms in Graphene Nanoplatelet Doped Polydimethylsiloxane and Application to Ultrasensitive Temperature Sensors,” *Cite This: ACS Appl. Mater. Interfaces*, vol. 15, 2023, doi: 10.1021/acsami.2c22162.

[29] S. Bhandari, Krishnanand, S. Roy, A. Singh, and M. Taufik, “Design and fabrication of accelerometer sensor using fused filament fabrication technique,” *Progress in Additive Manufacturing*, 2024, doi: 10.1007/s40964-024-00762-2.

[30] C. Chen *et al.*, “Next-generation health monitoring: The role of nanomaterials in 3D-printed wearable devices,” *Materials Today*, Mar. 2025, doi: 10.1016/J.MATTOD.2025.03.005.

[31] J. Han, Z. Li, S. Kong, S. Tang, D. Feng, and B. Li, “Wide-response-range and high-sensitivity piezoresistive sensors with triple periodic minimal surface (TPMS) structures for wearable human-computer interaction systems,” *Compos B Eng*, vol. 287, p. 111840, Dec. 2024, doi: 10.1016/J.COMPOSITESB.2024.111840.

[32] H. Yi, S. Wang, S. Mei, and Z. Li, “Conductive polymer composites for resistive flexible strain sensors,” *Polymer (Guildf)*, vol. 307, p. 127286, Jul. 2024, doi: 10.1016/J.POLYMER.2024.127286.

[33] S. Stankevich *et al.*, “Electrical Resistivity of 3D-Printed Polymer Elements,” *Polymers 2023, Vol. 15, Page 2988*, vol. 15, no. 14, p. 2988, Jul. 2023, doi: 10.3390/POLYM15142988.

[34] M. A. Ragolia, A. Di Nisio, A. M. Lanzolla, G. Percoco, M. Scarpetta, and G. Stano, “Thermal Characterization of Electrical Resistance of 3D printed sensors,” *Conference Record - IEEE Instrumentation and Measurement Technology Conference*, vol. 2021-May, May 2021, doi: 10.1109/I2MTC50364.2021.9459968.

[35] A. Gómez-Ortega, S. Piedra, G. C. Mondragón-Rodríguez, and N. Camacho, “Dependence of the mechanical properties of nylon-carbon fiber composite on the FDM printing parameters,” *Compos Part A Appl Sci Manuf*, vol. 186, p. 108419, Nov. 2024, doi: 10.1016/J.COMPOSITESA.2024.108419.

[36] M. F. Rabbi and V. Chalivendra, “Strain and damage sensing in additively manufactured CB/ABS polymer composites,” *Polym Test*, vol. 90, p. 106688, Oct. 2020, doi: 10.1016/J.POLYMERTESTING.2020.106688.

[37] J. Cañada and L. F. Velásquez-García, “Semiconductor-free, monolithically 3D-printed logic gates and resettable fuses,” *Virtual Phys Prototyp*, vol. 19, no. 1, Dec. 2024, doi: 10.1080/17452759.2024.2404157.